Vibrational autodetachment of sulfur hexafluoride anions at its long-lifetime limit

S. Menk,[1,*] S. Das,[2,†] K. Blaum,[1] M. W. Froese,[1] M. Lange,[1] M. Mukherjee,[2,†] R. Repnow,[1] D. Schwalm,[1,3] R. von Hahn,[1] and A. Wolf[1,‡]

[1]*Max-Planck-Institute for Nuclear Physics, Saupfercheckweg 1, 69117 Heidelberg, Germany*

[2]*Raman Center for Atomic Molecular and Optical Sciences, Indian Association for the Cultivation of Science, Kolkata 700 032, India*

[3]*Weizmann Institute of Science, Rehovot 76100, Israel*

(Received 14 June 2013; published 3 February 2014)

We have investigated the autodetachment of electrons from rovibrationally hot SF_6^- anions using a cryogenic ion-beam trap. Extremely low residual gas densities of 10^4 cm^{-3} provided undisturbed observation of the neutralization rates due to vibrational autodetachment (VAD) over almost five orders of magnitude and over times up to 100 ms. We successfully explain our experimental decay curves using statistical rate theory combined with electron attachment data and vibrational frequencies calculated for a C_{4v}-distorted SF_6^-. The unprecedented sensitivity of the experiment to the decay constants at the VAD threshold allows us to infer from the data the adiabatic electron affinity of SF_6 to be (0.91 ± 0.07) eV and to confirm the recently predicted C_{4v} symmetry of SF_6^-.

DOI: 10.1103/PhysRevA.89.022502 PACS number(s): 33.15.Ry, 34.80.Gs, 52.25.Tx

Owing to its large capture cross section for electrons [1], sulfur hexafluoride (SF_6) is commonly used in high-voltage equipments and accelerators as a gaseous dielectric and as a plasma etching gas [2]. For these applications [1] and also to understand the degradation [3] of the harmful greenhouse gas SF_6 from the Earth's atmosphere, the formation of SF_6^- anions and their destruction is of paramount interest. At low energies the formation usually proceeds via nondissociative attachment of an electron (e^-), thereby forming a rovibrationally excited SF_6^-, which in turn can undergo vibrational autodetachment (VAD) back to $SF_6 + e^-$ or radiative stabilization to states below the VAD threshold energy, i.e., the adiabatic electron affinity (EA) of SF_6.

Direct measurements of the VAD rates, performed by SF_6^- ion lifetime studies in vacuum [4–8], yielded results depending on the observation conditions. A subsequent ion storage ring experiment [9] found the neutralization signal $R(t)$ of SF_6^- to follow a power law for storage times up to a few milliseconds, $R(t) \propto t^n$, which indicates that a broad distribution of excited SF_6 states with different decay constants was contributing to $R(t)$ in the time range covered by the experiment [10]. This could rationalize the previously observed scattering of VAD rates. However, even in this high-vacuum measurement [9] the background SF_6^- neutralization signal due to residual gas collisions made it impossible to follow the VAD rate down to its lowest values occurring in the long-lifetime limit. A direct measurement of the VAD rate in this limit can be expected to reveal the influence of basic SF_6 and SF_6^- molecular parameters, such as the EA of the neutral and the SF_6^- vibrational level density at the detachment threshold. This appears timely considering the recently renewed discussion [11–14] of theoretical predictions on SF_6^- and appropriate methods to derive the SF_6 adiabatic EA from observations of the SF_6^- VAD.

Earlier experimental determinations [15,16] of the adiabatic electron affinity of SF_6 were based on thermodynamical methods and resulted in a recommended value of EA $= (1.06 \pm 0.06)$ eV [1]. More recently, an EA value of (1.20 ± 0.05) eV was deduced [11] from flowing afterglow measurements of thermal electron attachment and detachment rate constants by a third-law analysis using rovibrational partition functions calculated for an O_h-symmetric SF_6^- [17]. However, contrary to earlier findings, modern coupled-cluster (CC) calculations [13] predict the ground state of SF_6^- to have a C_{4v}-distorted geometry, which leads to far-reaching changes of its vibrational structure. Triggered by this finding, the experiment of Ref. [11] was reanalyzed by Troe *et al.* [12], now resulting in EA $= (1.03 \pm 0.05)$ eV, consistent with the previously recommended value but still larger than the *ab initio* CC result of 0.94 eV [13]. While corrections to the CC results were proposed [14], giving better agreement with the experimental results, the value of the SF_6 adiabatic EA and its influence on the VAD rates remain under debate.

Here we present VAD measurements of hot SF_6^- ions stored in the extremely high vacuum of the cryogenic electrostatic ion beam trap (CTF) [18] located at the Max-Planck-Institute for Nuclear Physics, which allowed us to observe the VAD signal down to rates almost three orders of magnitude lower than so far observable. We successfully reproduce our data using statistical rate theory when accounting for the C_{4v} distortion of SF_6^-. The present low-background measurement thus sensitively tests and confirms recent theories on the SF_6 electron collision dynamics and on the structure of the SF_6^- anion, and the detailed understanding of the VAD signals reached allows us to deduce the adiabatic electron affinity of SF_6.

Rovibrationally hot SF_6^- anions are created in a cesium sputter ion source [19] by feeding SF_6 through a 1 mm axial bore in a molybdenum cathode. The anions are produced by electron attachment presumably at the cesium-covered cathode surface. They are preaccelerated out of the source by the cathode voltage V_c (∼800–2000 V), which also guides the thermally ionized cesium ions from a heated tungsten filament towards the cathode. SF_6 pressures of up to ∼0.1 mbar are estimated in the SF_6^- production region, but fall steeply behind

*Present address: Atomic, Molecular and Optical Physics Laboratory, RIKEN, 2-1, Hirosawa, Wako-shi, Saitama 351-0198, Japan; sebastian.menk@riken.jp

†Present address: Centre for Quantum Technologies, National University Singapore, Singapore 117543.

‡A.Wolf@mpi-hd.mpg.de

the extraction aperture located at a distance of ∼2 cm from the cathode. Accelerated to 6 keV, the anions are chopped to bunches matching the revolution time in the CTF (∼20 μs), mass selected by a 90° deflection magnet, and injected into the cryogenic trap, where they oscillate between the two electrostatic mirrors [20]. For the present measurements, the CTF cooling circuit is supplied with 4.5 K helium gas, which cools the trapping region to 12–15 K, yielding an estimated residual gas density of order 10^4 cm^{-3}.

Fast neutral particles from VAD or from neutralization of SF_6^- by residual gas collisions can leave the trap through the central holes in the exit mirror electrodes and are counted by a microchannel plate (MCP) detector. These counts, recorded as a function of the storage time t and averaged over many injection cycles, yield the neutralization rate $R(t)$. As $R(t)$ is seen to be affected by small, irreproducible ion loss from the CTF during the first ∼15 ion oscillations (<300μs), only times $t \geqslant 1$ ms are considered in the following analysis. Moreover, at $t \geqslant 1$ ms it is also safe to neglect SF_6^- dissociation to $SF_5^- + F$, since ions with sufficient internal energies (>EA + 0.41 eV [12]) are expected to decay with lifetimes in the 10 μs range. Hence, we assume that $R(t)$ at $t > 1$ ms arises from VAD of SF_6^- only. However, additional contributions to the measured neutralization signal are due to residual gas collisions of SF_6^- and to a constant dark count rate of the MCP. The latter is regularly determined after dumping the SF_6^- ions and before starting a new injection cycle.

Figure 1 shows the extremely high contrast achieved in the present experiment between the neutralization of SF_6^- through VAD ($t < 0.1$ s) and that by residual gas collisions ($t > 0.1$ s). While in the previous storage ring experiment [9] the VAD signal was already obstructed after ∼10 ms by the residual gas contribution, we here can follow the VAD rate curve over almost five orders of magnitude up to unprecedented low decay rates occurring at decay times of ∼100 ms. As shown in Fig. 1, and in agreement with the findings of Rajput *et al.* [9], the VAD rates observed for dwell times $t \lesssim 5$ ms can be well represented by a power law. However, at higher t, where the neutralization rate is determined by SF_6^- states close to the autodetachment threshold, pronounced deviations from the power-law behavior are observed. In addition to short-time runs aiming at the observation of VAD, we also performed long-time measurements (up to $t = 400$ s) where the SF_6^- neutralization is due to residual gas collisions. By fitting an exponential decay law to the long-time data shown in the upper inset of Fig. 1 we deduced a storage lifetime of (800 ± 100) s.

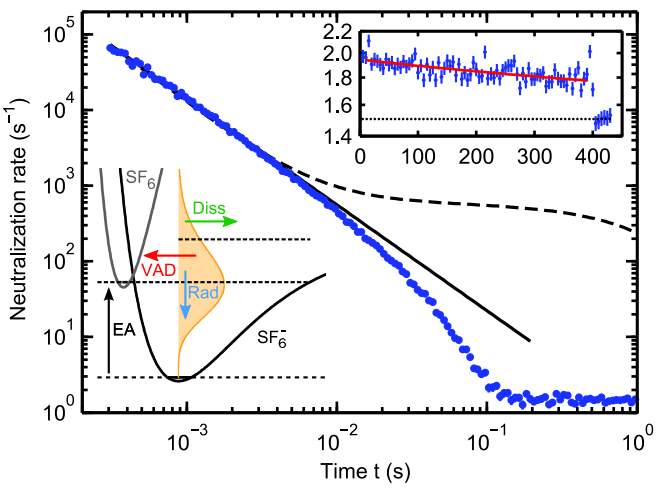

FIG. 1. (Color online) Measured neutralization rate $R(t)$ of SF_6^- as a function of the storage time t (dots). Previous storage ring data [9], rescaled in amplitude to match the present data, are shown for comparison (dashed line). The solid line is a fit of the present data for $t \leqslant 5$ ms by a power law ($\propto t^n$) with $n = -1.4$. Upper inset: Neutralization rate for long storage times (symbols) and exponential fit (solid curve). The dotted line represents the mean dark count rate of the MCP. Lower inset: Schematic ground state potential energy curves of SF_6^- and SF_6 as a function of a single S-F-bond distance and decay paths of excited SF_6^- ions (VAD: vibrational autodetachment, Diss: dissociation into $SF_5^- + F$, and Rad: radiative cooling).

Within the statistical approach the VAD neutralization rates of an ensemble of noninteracting SF_6^- ions with an initial distribution $f(E)$ of excitation energies E are given by (see, e.g., [10])

$$R_{\mathrm{VAD}}(t) = N_0 \int_{\mathrm{EA}}^{\infty} f(E)k(E)e^{-k_{\mathrm{tot}}(E)t}\,dE, \qquad (1)$$

where N_0 is the initial number of anions, $k_{\mathrm{tot}}(E)$ is the total decay rate coefficient, and $k(E)$ that for VAD. Unlike Refs. [9,21] we calculate the VAD rate coefficient $k(E)$ using statistical rate theory together with measured electron attachment cross sections, as recently elaborated by Troe *et al.* [12,22,23]. Moreover, we also take into account the rotation of the excited SF_6^- and SF_6, characterized by the total angular momentum J and its projection K onto the molecular symmetry axis. As the SF_6 electron attachment cross section $\sigma(\epsilon)$ for the relevant electron energies ϵ is dominated by s waves, the electron attachment (detachment) process can be assumed to preserve J and K. However, since the rotational constants of SF_6 and SF_6^- differ, the energy stored in the rotational motion changes in these processes. Neglecting the small K-dependent energy splitting in SF_6^-, the rotational energies of SF_6^- and SF_6 are approximated by $E_r^-(J) = J(J+1)\langle B^-\rangle$ and $E_r^0(J) = J(J+1)B^0$, respectively. Hence, an effective electron affinity can be introduced as $\mathrm{EA}(J) = \mathrm{EA} + E_r^0(J) - E_r^-(J)$. We adopt $B^0 = 0.0907$ cm^{-1} (O_h symmetry result [24] for SF_6) and $\langle B^-\rangle = 0.0753$ cm^{-1} (averaged constants A, B, and C as calculated for SF_6^- in C_{4v} symmetry [12]).

Following the detailed balance approach outlined in Ref. [22], the J specific VAD rate coefficients of an SF_6^- anion of total internal energy $E = E_v + E_r^-(J)$ are given by an integral over the electron energy ϵ,

$$k(E,J) = \frac{\mu}{\pi^2\hbar^3}\int_0^{E_v-\mathrm{EA}(J)} \frac{\sigma(\epsilon)\epsilon\,\rho_0\left(E_v^0(\epsilon)\right)}{\rho_-(E_v)}\,d\epsilon, \qquad (2)$$

where E_v is the energy stored in the vibrational degrees of freedom of SF_6^-, μ is the reduced mass of SF_6 and e^-, and $\rho_-(E_v)$ denotes the vibrational level density of SF_6^-. The vibrational energy remaining in the VAD decay product SF_6 is given by $E_v^0(\epsilon) = E_v - \mathrm{EA}(J) - \epsilon$, while $\rho_0(E_v^0)$ denotes the corresponding vibrational level density. Since the electron detachment threshold corresponds to a high vibrational excitation of SF_6^-, ρ_- can be approximated [22] by a smooth function using the Whitten-Rabinovitch approach

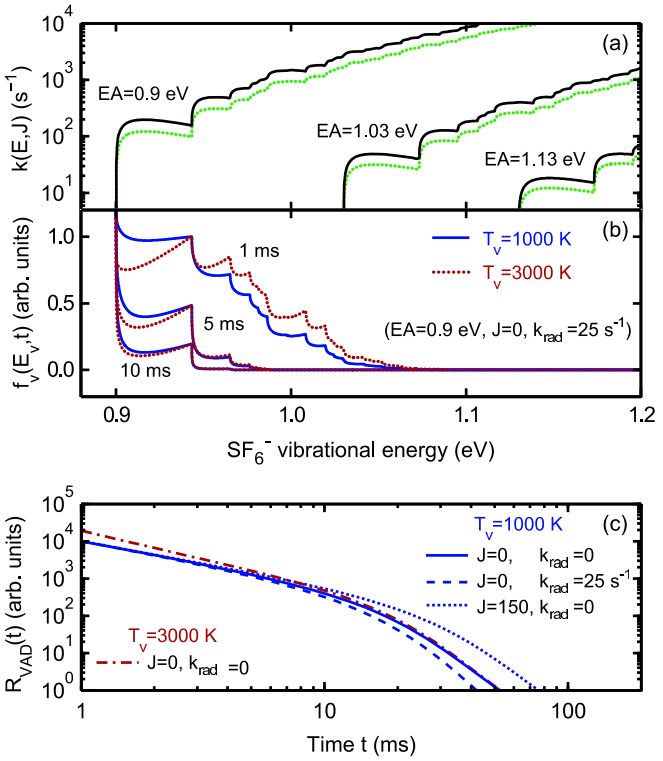

FIG. 2. (Color online) (a) VAD rate coefficients $k(E,J)$ from Eq. (2) for different EA, as functions of $E_v = E - E_r^-(J)$; solid lines for $J = 0$ and dotted lines for $J = 150$. (b) Vibrational energy distribution $f_v(E_v,t)$ of the stored SF_6^- ions for various storage times (labeled) and strongly different initial vibrational temperatures T_v ($J = 0$). The normalization was set to make the heights of the 1 ms curves match at the energy of the first vibrational level in SF_6 ($E_v^0 = 43$ meV). (c) VAD decay curves $R_{VAD}(t)$ from Eq. (3) with EA = 0.90 eV and different T_v, J, and k_{rad}.

[25]. On the other hand, at energies E lying only just above the detachment threshold, the vibrational states of SF_6 are sparse and the structure of ρ_0 calculated by the Beyer-Swinehart algorithm [26] is reflected in discrete contributions of these states to $k(E,J)$.

VAD rate coefficients $k(E,J)$ calculated with Eq. (2), using experimental attachment cross- sections [23] and level densities based on vibrational frequencies calculated most recently for a C_{4v}-symmetric SF_6^- [12,13], are shown in Fig. 2(a) for three values of EA. Each step in $k(E,J)$ occurring with increasing energy is due to the opening of new VAD channels provided by individual vibrational excitations in SF_6. The magnitude of $k(E,J)$ close to threshold strongly depends on EA, which results from the excitation energy dependence of the SF_6^- density of states $\rho_-(E_v)$ occurring in the denominator of Eq. (2). Increasing EA thus results in a decrease of $k(E,J)$, and as the effective EA(J) increases with J, higher J reduces $k(E,J)$. At their low-rate limit, the VAD rates become low enough that also competition with radiative emission of SF_6^- in the infrared (IR) needs to be considered. The radiative rates were estimated to lie at $\sim$60 s^{-1} [27] and, according to Fig. 2(a), can compete with VAD decays only at $E_v - \text{EA} \lesssim 50$–100 meV. These energies are similar to typical IR transition energies. Assuming that a single IR transition will result in $E_v < \text{EA}$ we can approximately include radiative cooling in Eq. (1) by setting $k_{tot} = k(E,J) + k_{rad}$.

As we observe many stored SF_6^- ions with insufficient internal energy for VAD, we conclude that these anions collisionally thermalize after their formation by electron attachment in the ion source. Hence, we choose a canonical vibrational energy distribution $f_v(E_v) \propto \rho_-(E_v)e^{-E_v/k_BT_v}$ with the vibrational temperature T_v and Boltzmann constant k_B, and a corresponding canonical rotational population distribution $f_r(J)$ with degeneracy $(2J+1)^2$ for a spherical top molecule at a rotational temperature T_r. The VAD decay curve of the excited SF_6^- ensemble is thus given by

$$R_{VAD}(t) = N_0 \sum_{J=0}^{\infty} f_r(J) \times \int_{EA(J)}^{\infty} f_v(E_v)k(E,J)e^{-[k(E,J)+k_{rad}]t}\,dE_v. \quad (3)$$

To illustrate the influence of these assumptions on the VAD decay curves, we show in Fig. 2(b) how the vibrational energy distribution of the stored SF_6^- ions develops in time. Here we set $f_v(E_v,t) \sim f_v(E_v,t=0)e^{-k_{tot}(E_v)t}$ with $k_{tot}(E_v) = k(E_v,0) + k_{rad}$. Although the initial distributions extend far above $E_v = \text{EA}$ (and much further for $T_v = 3000$ K than for $T_v = 1000$ K), already at $t = 1$ ms the populated states are essentially restricted to $E_v < \text{EA} + 0.2$ eV. For $t \geqslant 10$ ms the SF_6^- energy distributions above threshold become almost independent of the initial temperature, and the decay curves start to be dominated by states close to threshold. This is also displayed by the VAD decay curves $R_{VAD}(t)$ in Fig. 2(c), where the shapes of the two equivalent curves for $T_v = 1000$ and 3000 K almost agree for times $t > 10$ ms.

While the influence of the initial vibrational energy distribution onto the VAD decay curves dies out for $t \gtrsim 10$ ms, the high-J curve in Fig. 2(c) shows that $R_{VAD}(t)$ is still sensitive to the initial rotational distribution. Little is known about the rotational temperatures of molecules leaving a sputter ion source, but $T_r \gtrsim T_v$ may be expected [28], which translates into average J values of $\sim$150 for $T_r = 2000$ K. To show that we can consistently describe the observed VAD decay curves using Eq. (3), we changed the ion source parameters to vary T_r and T_v. Among the source parameters, the SF_6 pressure and the cathode voltage V_c were found to influence the shape of the $R_{VAD}(t)$ curves. We therefore performed high-statistics measurements of these curves at the extreme settings of $V_c = 800$ and 2000 V and for each V_c decreased the ion source pressure in five steps by throttling the SF_6 gas inlet and monitoring the pressure at the nearest downstream vacuum gauge. Example VAD decay curves for $V_c = 800$ V are displayed in Fig. 3, where a small constant background caused mainly by detector dark counts has been subtracted.

The ten observed VAD decay curves were fitted in the range 1 ms $\leqslant t \leqslant$ 200 ms using Eq. (3). For a given choice of the molecular parameters of the model, EA and k_{rad}, $R_{VAD}(t)$ was fitted to each of the ten curves, individually minimizing χ^2 by adjusting the temperatures T_v and T_r and the normalization N_0. This was repeated for a two-dimensional array in EA and k_{rad}, each time calculating the global χ^2/DOF of all ten curves, with DOF representing the relevant number of degrees of freedom

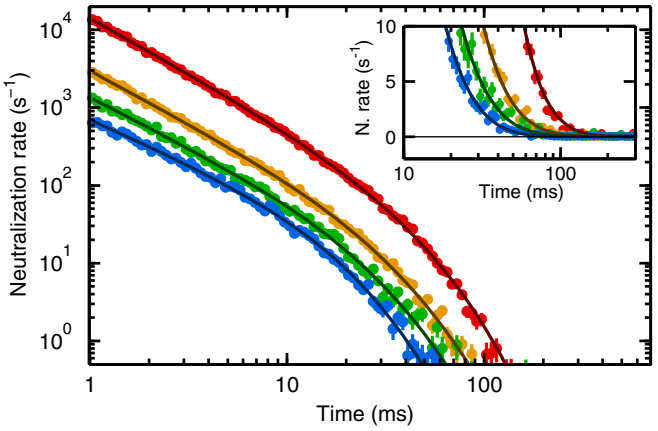

FIG. 3. (Color online) Background-subtracted VAD decay rates (symbols with statistical error bars) observed at four different SF_6 source pressures (highest to lowest pressures for top to bottom curves) and $V_c = 800$ V. Solid curves are fits of Eq. (3) using EA = 0.90 eV and $k_{rad} = 25\ s^{-1}$ and yielding T_v and T_r as shown in Fig. 4(b). Inset: Semilogarithmic plot of $R(t)$ for times $t > 10$ ms.

in all fits. This global reduced χ^2 is plotted in Fig. 4(a) as a function of EA and k_{rad} and assumes a well-defined minimum at $EA = 0.90^{+0.03}_{-0.05}$ eV and $k_{rad} = 25^{+3}_{-6}\ s^{-1}$ (1σ errors). The overall quality of the fit to the VAD curves at this minimum is illustrated by Fig. 3. The related best-fit temperatures T_v and T_r

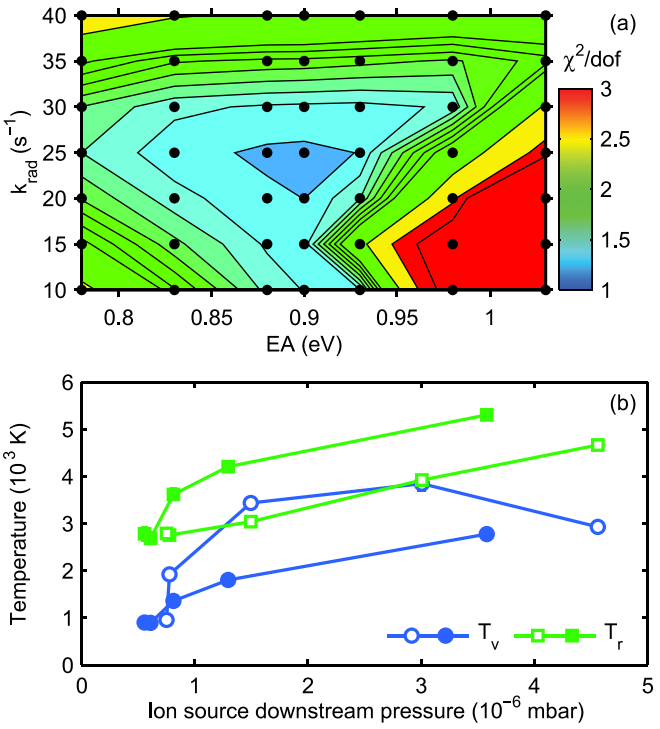

FIG. 4. (Color online) (a) Global reduced χ^2/DOF from the fits of all ten VAD decay curves over a grid (dots) of globally set EA and k_{rad} values, with the colors and contours obtained by interpolation. (b) Initial temperatures derived for vibrations (circles) and rotations (squares) from fits of the measured VAD decay curves with Eq. (3), setting EA = 0.90 eV and $k_{rad} = 25\ s^{-1}$. Full symbols: $V_c = 800$ V; open symbols: $V_c = 2000$ V.

are displayed in Fig. 4(b) showing their variation with the ion source downstream pressure for the two V_c settings; the absolute values span the range typical for sputter ion sources [28].

For minimizing the influence of the vibrational temperature, a corresponding fit was performed with the data at $10\ ms \leqslant t \leqslant 200$ ms only. It yielded $EA = (0.93 \pm 0.07)$ eV and $k_{rad} = 30^{+2}_{-8}\ s^{-1}$, well in agreement with the results for the full time range. We also investigated the influence of the one-step assumption leading to Eq. (3) by allowing the radiative transitions to proceed via a simplified cascade; while the EA value stays the same within its error, the effective radiative cooling constant k_{rad} is found to be slightly larger but a factor of almost smaller than the value estimated in Ref. [27]. The largest systematic error in the EA determination is expected from the accuracy of the vibrational level density $\rho_-(E_v)$ of SF_6^-; the distortion of SF_6^- from O_h towards C_{4v} symmetry not only results in the appearance of low-energy modes, but also in large anharmonicities which, so far, are only approximately accounted for [12]. This correction leads to a change of a factor of ~4 in $\rho_-(E_v)$, the accuracy of which we estimate to be only ±2. This transforms into an error in the EA of ±0.05 eV. Note, however, that we cannot reproduce our data using SF_6^- vibrational level densities based on O_h frequencies, even allowing for unreasonable small k_{rad} values and unreasonable large initial temperatures. Combining our results and error estimates, we finally infer from our measurements $EA = (0.91 \pm 0.07)$ eV for the electron attachment energy of SF_6, and $k_{rad} = (27 \pm 6)\ s^{-1}$ for the effective radiative cooling constant of SF_6^- around EA.

In conclusion, the low-background conditions in the cryogenic ion beam trap have allowed us to investigate the VAD process of excited SF_6^- anions in the so far not accessible long-time and low-intensity limit. Using statistical rate theory together with experimental electron attachment data and improved structure information for SF_6^-, we arrive at a consistent description of the VAD decay rates over almost five orders of magnitude. We find that the distorted ground-state geometry of SF_6^- predicted by a recent model calculation [13] is essential for achieving this consistency. The deduced value for the adiabatic electron attachment energy of $EA(SF_6) = (0.91 \pm 0.07)$ eV is smaller, but still consistent within errors with the most recent experimental value of (1.03 ± 0.05) eV by Troe *et al.* [12]. Moreover, our value is in excellent accord with the theoretical prediction of 0.94 eV by Eisfeld [13], but in less good agreement when recently proposed corrections [14] are applied to the CC result. The present study shows the power of cryogenic ion beam storage devices to analyze VAD rates for complex molecular systems in the range where they are small but closely reflect basic molecular properties.

We thank J. Troe and W. Eisfeld for helpful discussions. S.M. acknowledges support from the Alliance Program of the Helmholtz Association (HA216/EMMI), M.M. and S.D. acknowledge the support by DST (India) and MPG (Germany) under the scheme of DST-MPI international fellowship (INT/FRG/MPG/FS(3)/2009), and D.S. acknowledges support by the Weizmann Institute of Science through the Joseph Meyerhoff program. Financial support by the Max-Planck Society and the Max-Planck Förderstiftung is acknowledged.

[1] L. G. Christophorou and J. K. Olthoff, J. Phys. Chem. Ref. Data **29**, 267 (2000).
[2] M. Braun, S. Marienfeld, M.-W. Ruf, and H. Hotop, J. Phys. B: At., Mol. Opt. Phys. **42**, 125202 (2009).
[3] T. Reddmann, R. Ruhnke, and W. Kouker, J. Geophys. Res. **106**, 14525 (2001).
[4] D. Edelson, J. Griffiths, and K. McAfee, Jr., J. Chem. Phys. **37**, 917 (1962).
[5] R. Odom, D. Smith, and J. Futrell, J. Phys. B: At. Mol. Phys. **8**, 1349 (1975).
[6] A. D. Appelhans and J. E. Delmore, J. Chem. Phys. **88**, 5561 (1988).
[7] J.-L. Le Garrec, D. A. Steinhurst, and M. A. Smith, J. Chem. Phys. **114**, 8831 (2001).
[8] Y. Liu, L. Suess, and F. B. Dunning, J. Chem. Phys. **122**, 214313 (2005).
[9] J. Rajput, L. Lammich, and L. H. Andersen, Phys. Rev. Lett. **100**, 153001 (2008).
[10] J. U. Andersen, E. Bonderup, and K. Hansen, J. Phys. B: At. Mol. Opt. Phys. **35**, R1 (2002).
[11] A. A. Viggiano, T. M. Miller, J. F. Friedman, and J. Troe, J. Chem. Phys. **127**, 244305 (2007).
[12] J. Troe, T. M. Miller, and A. A. Viggiano, J. Chem. Phys. **136**, 121102 (2012).
[13] W. Eisfeld, J. Chem. Phys. **134**, 054303 (2011); **134**, 129903 (2011).
[14] A. Karton and J. M. L. Martin, J. Chem. Phys. **136**, 197101 (2012).
[15] E. P. Grimsrud, S. Chowdhury, and P. Kebarle, J. Chem. Phys. **83**, 1059 (1985).
[16] E. C. M. Chen, J. R. Wiley, C. F. Batten, and W. E. Wentworth, J. Phys. Chem. **98**, 88 (1994).
[17] G. L. Gutsev and R. J. Bartlett, Mol. Phys. **94**, 121 (1998).
[18] M. Lange, M. Froese, S. Menk, J. Varju, R. Bastert, K. Blaum, J. R. Crespo López-Urrutia, F. Fellenberger, M. Grieser, R. von Hahn, O. Heber, K.-U. Kühnel, F. Laux, D. A. Orlov, M. L. Rappaport, R. Repnow, C. D. Schröter, D. Schwalm, A. Shornikov, T. Sieber, Y. Toker, J. Ullrich, A. Wolf, and D. Zajfman, Rev. Sci. Instrum. **81**, 055105 (2010).
[19] R. Middleton, Nucl. Instrum. Methods Phys. Res. **214**, 139 (1983).
[20] D. Zajfman, O. Heber, L. Vejby-Christensen, I. Ben-Itzhak, M. Rappaport, R. Fishman, and M. Dahan, Phys. Rev. A **55**, R1577 (1997).
[21] L. H. Andersen, Phys. Rev. A **78**, 032512 (2008).
[22] J. Troe, T. M. Miller, and A. A. Viggiano, J. Chem. Phys. **130**, 244303 (2009).
[23] H.-J. Troe, G. Marowsky, N. S. Shuman, T. M. Miller, and A. A. Viggiano, Z. Phys. Chem. **225**, 1405 (2011).
[24] M. W. Chase, Jr., *NIST-JANAF Thermochemical Tables*, 4th ed., J. Phys. Chem. Ref. Data, Monograph 9 (AIP, New York, 1998), p. 1205, http://www.nist.gov/srd/monogr.cfm.
[25] G. Z. Whitten and B. S. Rabinovitch, J. Chem. Phys. **38**, 2466 (1963).
[26] T. Beyer and D. F. Swinehart, Commun. ACM **16**, 379 (1973).
[27] J. Troe, T. M. Miller, and A. A. Viggiano, J. Chem. Phys. **127**, 244303 (2007).
[28] A. Wucher and B. Garrison, J. Chem. Phys. **105**, 5999 (1996).